

# NUMERICAL MODEL FOR THE MINIMIZATION OF INTERMIXED ROUND BARS IN A FOUR LINE CONTINUOUS CASTER

Marcela B. Goldschmit<sup>\*</sup>, Sergio P. Ferro<sup>\*</sup>, Guillermo F. Walter<sup>+</sup>,

Virginia G. Aranda<sup>+</sup> and Jorge A. Tena Morelos<sup>+</sup>

<sup>\*</sup> Center for Industrial Research (CINI)  
Fundación para el Desarrollo Tecnológico (FUDETEC)  
Córdoba 320, 1054 Buenos Aires, Argentina  
e-mail: sidgld@siderca.com  
<sup>+</sup>SIDERCA S.A.I.C.  
Dr. Simini 250, 2804 Campana, Argentina

**Abstract.** *The grade transition process in a four lines round billets continuous caster was analysed. A numerical model able to determine fast and accurately the length and location of intermixed steel in the bar was developed. The model is based on “tank in series” or “volumes” mathematical models and was calibrated with physical water model measurements and full 3D turbulent numerical calculations. Comparison of the model with measurements performed on intermixed steel bars are also presented. The good agreement between these plant measurements and the numerical results validated the model. The model was implemented on PCs with a visual interface which allows the easy input and output of data, and the program is operating in the steel shop. Finally, the code was employed to evaluate different strategies to fill the tundish during grade transits. The “double dilution” process, which consists in filling the tundish in two steps, proved to be useful to reduce the amount of downgraded steel.*

## I. INTRODUCTION

Sequential casting of different steel grades during continuous casting process is often employed in steel plants in order to maximise the productivity of the caster. This procedure, however, generates an amount of mixed steel which does not satisfy the required specifications and must be downgraded. The motivation of the present work is to develop a numerical model of the chemical composition of the steel bars during a grade transition and provide an estimation of the position and length of the bars of intermixed steel.

Transition grade models<sup>[1-6]</sup> have been published in the literature since 1992. Numerical models, physical water models and experimental studies were employed to address the problem. Most publications have considered grade transitions with only two continuous casting lines, casters with more than two lines being rare in literature<sup>[7]</sup>.

Several works in literature<sup>[1,8-9]</sup> showed grade transition models with focus on mixing in the tundish. Diener, Pluschkell and Sardeman<sup>[10]</sup> introduced the mixing in the mold in the transition models and Huang and Thomas<sup>[2]</sup> introduced the mixing in the strand.

Works<sup>[1-10]</sup> made the grade transition models with “tank in series” mathematical models also called “box models” or “volume models”. All these models, however, consider a one-step filling of the tundish, with the tundish volume increasing monotonically till its operating value.

The aim of this work is to develop a numerical model which can predict the location of the intermixed steel in a four line-round caster in a fast and accurate way, for a wide variety of casting conditions including time dependent casting speed and time dependent inlet flow rate. This model could be used to optimise the casting conditions during a grade change, to find the best sequence of grades to be casted and to specify the points where the bars should be cut. All these improvements tend to reduce the intermix costs when different grades are casted in single sequence. By estimating these costs, the model also helps to decide when a tundish change is convenient. The model focuses on the four line round billet caster used at Siderca, but it can be easily modified to be applied to more general situations.

The model consists of three sub-models. One associated to the tundish, which was tested and calibrated with water model measurements performed by IAS<sup>[11]</sup>. A second one associated with the mold and upper part of the bar, which was calibrated with a 3D numerical k- $\epsilon$  turbulent model using a (k-L)-predictor /( $\epsilon$ )-corrector iterative algorithm. This was addressed in our previous publications<sup>[12-13]</sup>. This numerical algorithm was used to model some processes in the continuous casting<sup>[14-16]</sup>. The last one associated with the final composition in the bar, solves a convection-diffusion equation (with the

turbulent diffusivity estimated by the 3D model). The model was implemented in our user friendly code GRADE<sup>[21]</sup>.

The description of the model is presented in detail in sections two, three and four. In Section five, plant measurements of intermixed steel composition made in SIDERCA Steel plant, which validate the numerical model, are shown. Different dilution strategies of two steel grades are shown in Section six. The last Section is devoted to the conclusions.

## II. MODELING CRITERIA

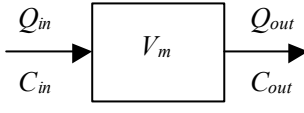
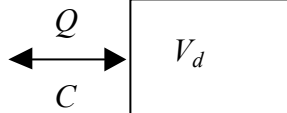
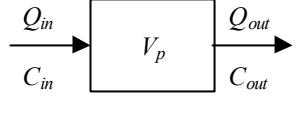
An important point to keep in mind is that, as the flow is highly turbulent, the turbulent diffusivity is much greater than the molecular one. Consequently, all chemical species will show the same behaviour. This was confirmed by plant measurements described in Section V. Thus, concentration calculations were performed for a single dimensionless function ( $\tilde{C}(t)$ ) defined by

$$\tilde{C}(t) = \frac{C(t) - C_{old}}{C_{new} - C_{old}} \quad [1]$$

where  $C_{old}$  and  $C_{new}$  represent the concentration of a given element in the old and new steel grade respectively. This dimensionless concentration can take any value between 0 (old steel grade) and 1 (new steel grade). Once the dimensionless concentration is calculated, the concentration of a given chemical element ( $C(t)$ ) may be obtained from Eq. [1].

The model is composed by three types of volumes: mixing volume, dead volume and plug volume. The basic equations of the model may be derived by imposing mass conservation for the fluid and for the chemical elements on each volume. Mixing volumes are assumed to be well mixed, having a uniform concentration equal to the outcoming one for each time interval. Plug flow volumes introduce a delay ( $t_p$ ) in the outcoming concentration. In Table I we show the description and the equations for the three volumes.

**Table I. Description of the basic volumes**

Equation	Mixing volume ( $V_m$ )	Dead volume ( $V_d$ )	Plug volume ( $V_p$ )
			
Mass conservation	$\frac{dV_m}{dt} = Q_{out} - Q_{in}$	$\frac{dV_d}{dt} = \pm Q$	$\frac{dV_p}{dt} = Q_{out} - Q_{in}$
Mass conservation of a chemical elements	$\frac{dC_{out}}{dt} = \frac{Q_{in}}{V_{in}}(C_{in} - C_{out})$	$C \neq f(Q, V)$	$C_{out} = C_{in} \left( t - \frac{V_p}{Q_{in}} \right)$

The time  $t = 0$  is considered when the ladle with the new steel grade is opened.

The model consists of three sub-volume models: tundish, mold and final composition.

### III. TUNDISH MIXING MODEL

#### A. Volumes model

The flow inside the tundish was modelled by a “tank in series” mathematical model. Several “tanks” or “volumes” were considered to model a four line symmetric tundish with isothermal flow. In Figure 1 we show the mixing volume model of half the tundish with the internal and external continuous casting lines.

There are two well defined groups of volumes: one of them associated with the internal lines (superscript *int*) and the other associated with the external lines (superscript *ext*); with an extra recirculating mixing volume ( $V_m^R$ ) which allows the mass flow between both groups of volumes.

Each of these groups consists of two mixing volumes ( $V_{m1}$  and  $V_{m2}$ ), one dead volume ( $V_d$ ), and one plug flow volume ( $V_p$ ).

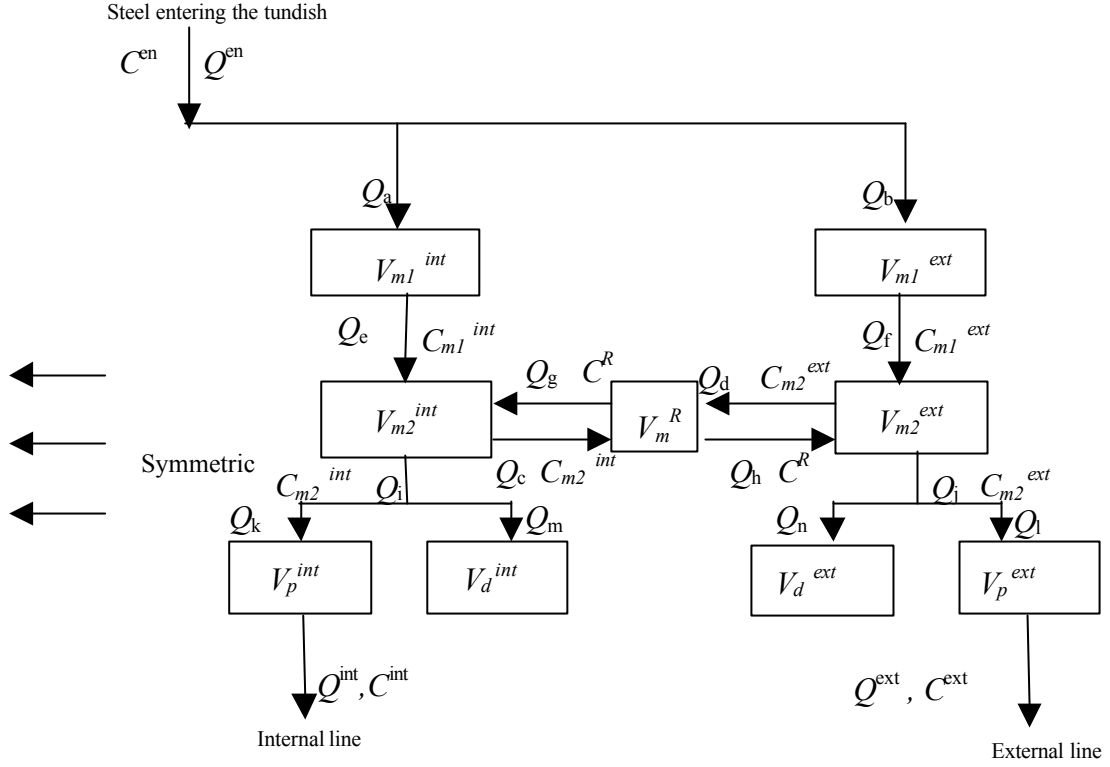


Fig. 1--Tundish mixing model

## B. Equations

Using the basic equations previously described in Table I and assembling them according to Figure 1, we reach the following system of equations,

$$\begin{aligned}
 Q_a &= x_a Q^{en} & Q_b &= Q^{en} - Q_a \\
 Q_e &= Q_a - dV_{m1}^{int}/dt & Q_f &= Q_b - dV_{m1}^{ext}/dt \\
 Q_k &= Q^{int} + dV_p^{int}/dt & Q_l &= Q^{ext} + dV_p^{ext}/dt \\
 Q_m &= dV_d^{int}/dt & Q_n &= dV_d^{ext}/dt \\
 Q_i &= Q_k + Q_m & Q_j &= Q_l + Q_n \\
 Q_c &= x_c Q_i & Q_d &= x_d Q_j \\
 Q_g &= Q_c + Q_i - Q_e + dV_{m2}^{int}/dt & Q_h &= Q_d + Q_j - Q_f + dV_{m2}^{ext}/dt \\
 C^{int} &= C_{m2}^{int}(t-t_p^{int}) & C^{ext} &= C_{m2}^{ext}(t-t_p^{ext}) \\
 dC_{m1}^{int}/dt &= Q_a(C^{en} - C_{m1}^{int})/V_{m1}^{int} & dC_{m1}^{ext}/dt &= Q_b(C^{en} - C_{m1}^{ext})/V_{m1}^{ext} \\
 dC_{m2}^{int}/dt &= (Q_e C_{m1}^{int} + Q_g C^R - (Q_g + Q_e) C_{m2}^{int})/V_{m2}^{int} \\
 dC_{m2}^{ext}/dt &= (Q_f C_{m1}^{ext} + Q_h C^R - (Q_f + Q_h) C_{m2}^{ext})/V_{m2}^{ext} \\
 dC^R/dt &= (Q_d C_{m2}^{ext} + Q_c C_{m2}^{int} - (Q_d + Q_c) C^R)/V_m^{ext}
 \end{aligned} \tag{2}$$

In this system of equations the volume fractions  $f_i = V_i / V_T$ , are parameters to be calibrated with the water model. The total flow rate entering ( $Q^{en}$ ) and leaving ( $Q^{int} + Q^{ext}$ ) the tundish are known functions of time, which the user must specify. In consequence the half-tundish volume ( $V^T$ ) is also a known function of time.

There are three flow rate fractions to be calibrated:

$$x_a = \frac{Q_a}{Q^{en}} \quad (\text{fraction of entering flow rate directed to the internal line});$$

$$x_d = \frac{Q_d}{Q_j} \quad (\text{fraction between the two flow rates coming out of } V_{m2}^{ext}); \text{ and}$$

$$x_c = \frac{Q_c}{Q_i} \quad (\text{fraction between the two flow rates coming out of } V_{m2}^{int}).$$

The new grade composition prescribes the concentration of the chemical elements at the tundish entrance,  $C^{en}$ . The time delay introduced by the plug flow volumes is given by  $t_p^{int} = V_p^{int} / Q_k^{int}$  and  $t_p^{ext} = V_p^{ext} / Q_l^{ext}$ .

The system of coupled ordinary differential equations was solved with a fourth order Runge Kutta algorithm, with the old grade composition as initial composition.

### C. Water model calibration

The tundish model just described was calibrated with experimental measurements performed by IAS<sup>[11]</sup> on a physical water model. The water model is a 1:3 scale reproduction of the tundish at Siderca S.A.I.C. (Campana, Argentina), which is 14 tons in weight and is equipped with an impact pad. The experience simulated a constant velocity of 2.1 m/min in each continuous casting lines of bars with a diameter of 0.140 m.

The tracking of the concentration was accomplished by injecting a salt solution into the tundish entrance and analysing the flow coming out of each line for different time instants.

The residence time distribution (RTD) curves are presented in Figure 2. The time is represented in terms of the theoric mean residence time  $\hat{t} = tQ^{en} / V_T$ ,  $t = 0$  being the moment when the salt solution was injected. The non dimensional concentration in this Figure was defined in such a way that the area

beneath the inner-line curve is the unity,  $\hat{C} = C / \int_0^\infty C(\hat{t}) d\hat{t}$ .

To find out the group of parameters which best fits the RTD curves obtained by the water model experience, the function  $\sum_k (C_{int}(t_k) - C_{int}^{wm}(t_k))^2 + (C_{ext}(t_k) - C_{ext}^{wm}(t_k))^2$  was considered. In this expression, the superscript *wm* indicates concentrations obtained by the water model experience and the  $t_k$  are time intervals where the concentrations were evaluated. The parameter space was explored in order to find the set of parameters that minimises this function.

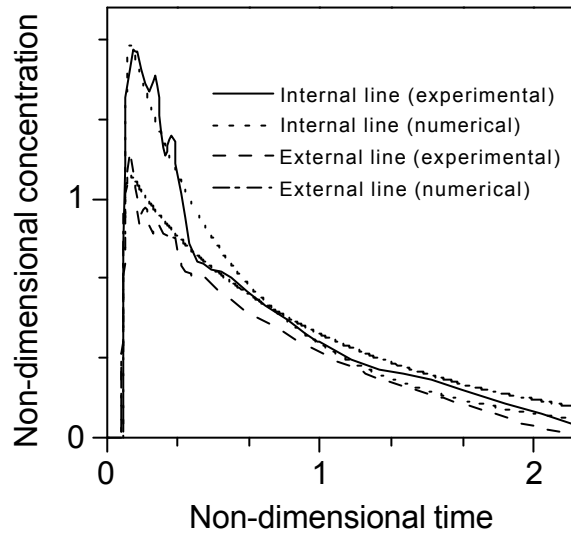


Fig. 2--Calibration of the tundish mixing model

The resulting parameters were:

$$\begin{aligned}
 f_{m1}^{ext} = f_{m1}^{int} &= 0.0004 & f_{m2}^{int} &= 0.33 & f_{m2}^{ext} &= 0.44 \\
 f^* &= 0.08 & f_p^{int} &= 0.04 & f_p^{ext} &= 0.035 \\
 f_{d1}^{ext} = f_{d2}^{int} &= 0.0371 & x_a &= 0.53 & x_d = x_c &= 0.36
 \end{aligned} \tag{3}$$

The non-dimensional concentrations obtained by setting these parameters in the numerical model are plotted in Figure 2.

#### D. Simple and double dilution

During normal operation, the steel weight in the tundish is kept almost constant at a certain value

$W_{tundish}$ . Under this condition, the flow rate entering the tundish  $Q_{steady}$  equals the flow rate leaving the tundish through its four lines. This flow rate is given by the casting speed and the bar diameter. When a ladle change takes place, no steel enters the tundish and the steel weight in the tundish is reduced to a minimum value  $W_{drain}$ . The filling of the tundish could be carried out in two different ways:

- *Simple dilution procedure:* When the new ladle opens, the flow rate entering the tundish is set to a value  $Q_{sd}$  above  $Q_{steady}$  till the operating weight  $W_{tundish}$  is reached. Then the caster is in normal operation again, with  $W_{tundish}$  and  $Q_{steady}$ . Figure 3 shows the time evolution of the weight of steel in the tundish and the inlet flow rate when a simple dilution procedure is adopted to fill the tundish.
- *Double dilution procedure:* The filling of the tundish is performed in two steps, as depicted in Figure 4. When the ladle with the new grade opens, it fills the tundish only up to a certain weight  $W_1$  with a flow rate  $Q_{dd}^1$ . Then it closes for a while (in fact it is not completely closed, a little flow rate  $Q_{dd}^2$  still entering the tundish), allowing for a second draining of the tundish. When a second minimum steel weight  $W_{drain2}$  is attained, the ladle opens again with  $Q_{dd}^3$  flow rate, for the tundish to reach the operating weight  $W_{tundish}$ . Then the flow rate is reduced to the steady state value  $Q_{steady}$ , in order to keep a constant steel weight in the tundish.

The time duration of each step is determined by the weight and the flow rate entering and leaving the tundish.

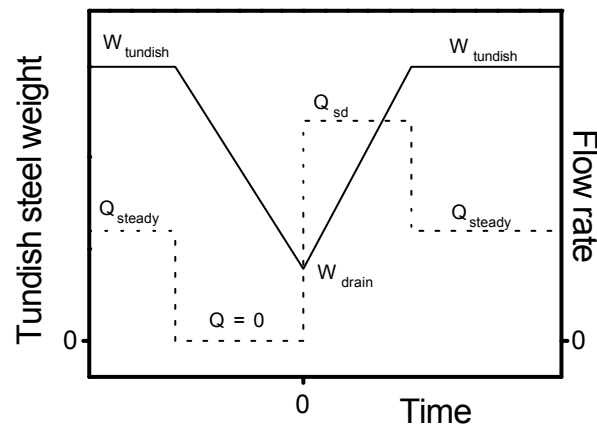


Fig. 3--Scheme of a simple dilution procedure. Full lines indicate the weight of the steel in tundish and dotted lines the flow rate of the steel entering the tundish.



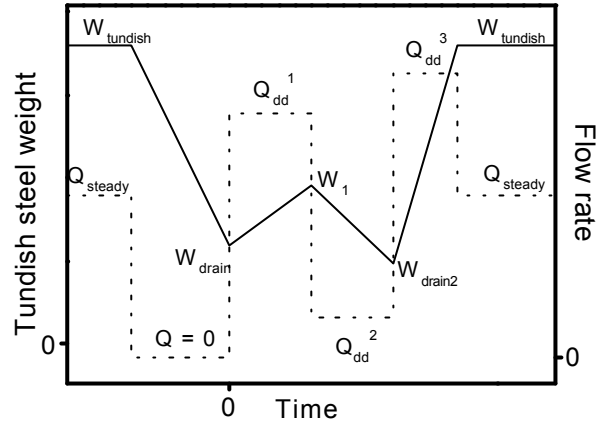


Fig. 4--Scheme of a double dilution procedure. Full lines indicate the weight of the steel in tundish and dotted lines the flow rate of the steel entering the tundish.

#### IV. MOLD MIXING MODEL AND FINAL COMPOSITION

##### A. Volumes model

The model in the mold and upper part of the bars considers the first three meters of fluid below the meniscus. It was validated with a numerical full 3D turbulence model<sup>[12-16]</sup> and consists of a plug flow volume and a mixing volume, followed by a region where convective and diffusive effects were supposed to take place (see Figure 5). In this latter region a one dimension convection-diffusion equation was solved with the co-ordinate  $z$  (taken along the bar) being the only relevant variable.

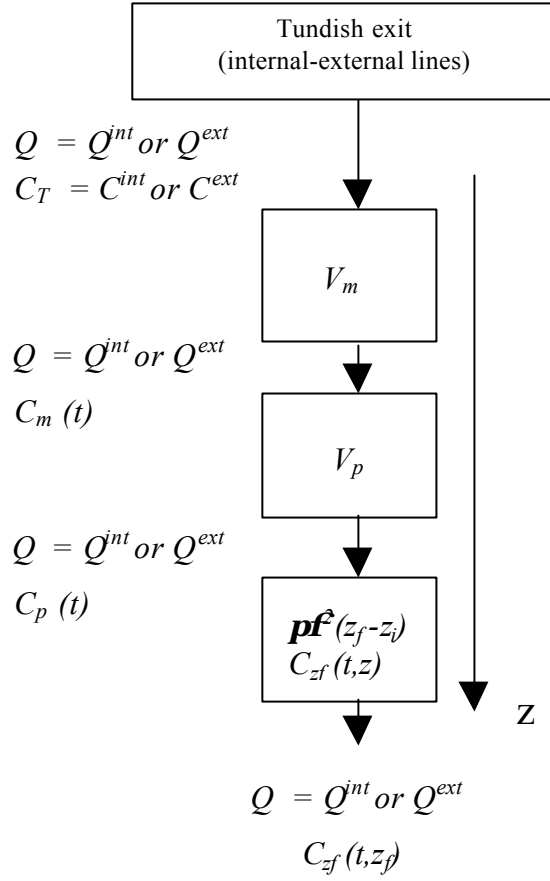


Fig. 5--Mold mixing model

The following set of equations for the concentration is obtained,

mixing volume

$$\frac{dC_m}{dt} = \frac{Q}{V_m} (C_T - C_m)$$

plug flow volume

$$C_p = C_m \left( t - \frac{V_p}{Q} \right) \quad [4]$$

convection-diffusion region

$$\frac{\partial C_{zf}}{\partial t} + v_z \frac{\partial C_{zf}}{\partial z} = \frac{\partial}{\partial z} \left( D_{eff} \frac{\partial C_{zf}}{\partial z} \right) ; \quad z_i < z < z_f$$

where  $V_m$  is the mold mixing volume;  $V_p$  is the mold plug flow volume;  $C_m$ ,  $C_p$ , and  $C_{zf}$  are the concentrations exiting each region;  $v_z$  is the casting speed;  $D_{eff}$  is the turbulent diffusivity;  $z_i = (V_m + V_p)/\mathbf{pf}$  and  $z_f$  are the initial and final positions of the convection-diffusion region; and  $\mathbf{f}$  is the bar radius.

The values of  $Q$  and  $C_T$  are taken from the tundish mixing model, while the values of  $V_m$ ,  $V_p$ , and  $D_{eff}$  are estimated by calibration with results obtained with a numerical 3D turbulent model<sup>[12-16]</sup>, as described below.

#### B. Validation with a 3D finite element model

The mold mixing model was calibrated in the following way:

- ✓ The steel flow inside the system nozzle-mold-bar was numerically calculated using a 3D code<sup>[17]</sup>. This code solves the  $k$ - $\epsilon$  turbulent flow equation using a  $(k$ - $L$ )-predictor /  $(\epsilon$ -corrector iterative algorithm. This was addressed in our previous publications<sup>[12-16]</sup>. These calculations were performed considering different casting speeds and mold diameters. The modelled domain includes the nozzle, the mold and part of the bar until three meters below the meniscus.
- ✓ Once the velocity field was obtained, the transport equation for a chemical element in a turbulent stream was calculated by solving a transient turbulent convection-diffusion equation:

$$\frac{\partial c}{\partial t} + \underline{v} \cdot \underline{\nabla} c = \underline{\nabla} \cdot [(D + D^t) \underline{\nabla} c] \quad [5]$$

where  $c$  is the time averaged concentration for a chemical specie;  $\underline{v}$  is the time averaged velocity;  $D$  is the molecular diffusivity for the specie; and  $D^t$  is the turbulent diffusivity.  $D^t$  was considered equal to the turbulent dynamic diffusivity  $D^t = \frac{\underline{m}}{\underline{r}}$  ( $\underline{m}$ : turbulent viscosity given by the  $k$ - $\epsilon$  model,  $\underline{r}$ : density) and  $D \ll D^t$ . Therefore, all species have the same concentration distribution behaviour.

Eq. [5] is integrated with the Streamline Upwind Petrov Galerkin technique<sup>[18-19]</sup> and a standard 8-node (3D) isoparametric finite element discretization<sup>[20]</sup> for  $c$ .

Free parameters of the 1D model were calibrated with the concentration obtained by these 3D calculations. The following values were found:

$$V_m = \underline{pf}^2 \times 0.5 \text{ m} \quad ; \quad V_p = \underline{pf}^2 \times 1.06 \text{ m} \quad ; \quad D_{eff} \approx 30 \text{ mm}^2 / \text{seg}$$

Figure 6 shows the dimensionless concentration distribution for different time intervals in the

azimuthal plane. This figure was obtained in a simulation with a casting speed of 2 m/min, a mold diameter of 0.170 m. The concentration imposed at the nozzle was given by the tundish model, supossing a typical double dilution process and that corresponds to an external line.

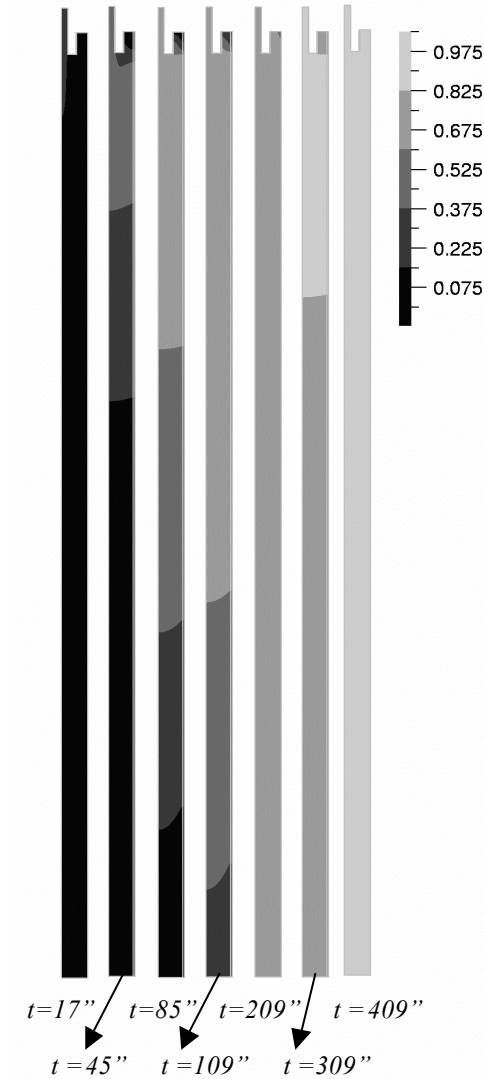


Fig. 6--Concentration in the system nozzle-mold-bar for different time instants

Results from the 3D numerical model show an almost one dimensional flow below a distance of 1.5 m from the meniscus. In Figure 7 the dimensionless concentration at 1.56 m below meniscus is plotted as function of time. In this figure, lines correspond to 1D model results and symbols to 3D model results.

The good agreement observed validates the use of the 1D model. The abrupt slope change in both lines is due to the double dilution process already stated.

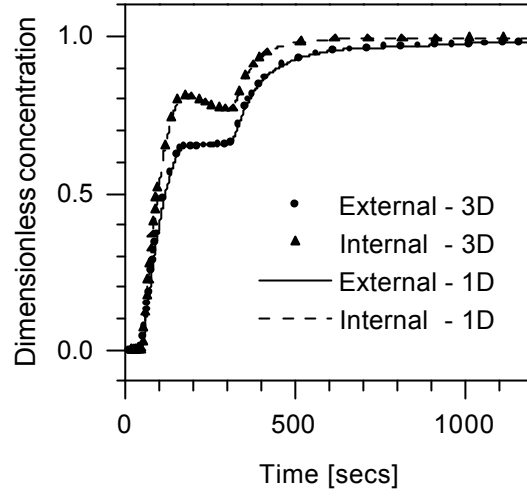


Fig. 7--Comparison of dimensionless concentration at 1.56 m below meniscus as given by the 1D volumes model and the 3D turbulent model

#### C. Final composition of the bar

The third submodel solves the convection diffusion equation (Eq. [5]) using the turbulent diffusivity given by the 3D numerical model, in a region between the 1.56 m below meniscus and the solidification point. Diffusion in solid state is neglected.

The solidification point would be different for each point of the bar cross section depending on its distance to the surface.

The complete solution of Eq. [5] proved that diffusive effects can also be neglected in the liquid pool. This is due to the low values of the turbulent diffusivity in the lower part of the line, and was verified by direct measurements of steel composition performed in plant (see Figure 8).

Consequently, the composition along the bar was calculated by convection of the elements concentration due to the casting speed and was considered homogeneous across the bar section.

#### D. Final calculations

Having calibrated the model, a numerical code (GRADE<sup>[21]</sup>) was developed. The code calculates the dimensionless concentration  $\tilde{C}(t)$  at the cutoff point of the bar, as function of time.

The user is supposed to provide the following input data:

- Casting speed as piecewise function of time in each casting line.
- Flow rate entering the tundish as piecewise function of time.
- Concentration of each element in the old and new grade.
- Specification of the composition of both steel grades.
- Diameter of the bar

With this information, the program is able to detect the old grade / intermixed steel boundary and the new grade / intermixed steel boundary in the bar at the cut-off point.

The program also calculates the proportion of new grade steel and old grade steel in the intermixed bar which is needed to estimate the cost of the downgraded steel.

## V. COMPARISON WITH PLANT MEASUREMENTS

The final validation of the model was accomplished by direct composition measurements of round billets from Siderca S.A.I.C. continuous caster. Two different changes of grade were analysed, the first one having B as critical element, the second one having Cr as critical element.

In both cases, the filling of the tundish (after the drainage due to the ladle change) was performed in a double dilution process. This process is the standard procedure adopted by Siderca.

### A. Plant measurements – Example A

The first set of measurements to be analysed corresponds to a grade transition determined by the casting conditions of Table II and the chemical composition of Table III.

**Table II. Casting conditions of Example A**

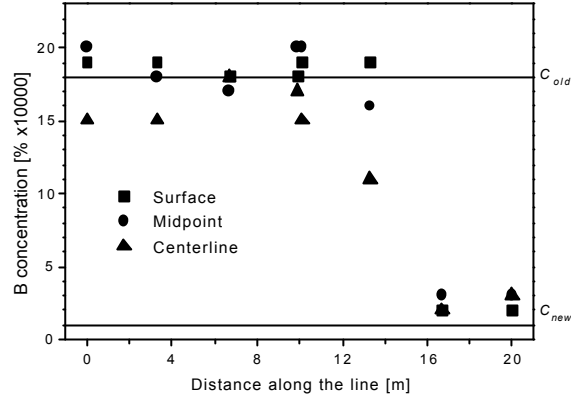
$W_{tundish}$	15.4 tons
$W_{drain}^1$	3.0 tons
$W^1$	6.0 tons
$W_{drain}^2$	4.0 tons
$Q_{steady}$	1.3 ton/min
$Q_{dd}^1$	3.05 ton/min
$Q_{dd}^2$	0.57 ton/min
$Q_{dd}^3$	3.56 ton/min
Bar diameter	0.170 m
Casting speed	2 m/min

**Table III. Chemical composition of Example A**

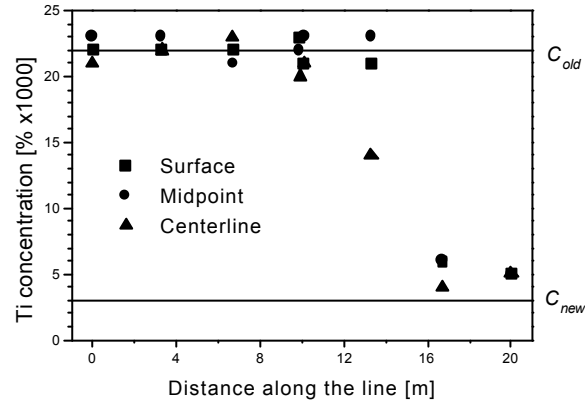
Element	Old Grade			New Grade		
	Minimum	Maximum	Actual	Minimum	Maximum	Actual
C	0.24	0.27	0.26	0.27	0.3	0.29
Mn	1.3	1.45	1.33	1.25	1.4	1.31
S	0	0.01	0.002	0	0.01	0.006
P	0	0.025	0.016	0	0.02	0.019
Si	0.25	0.35	0.29	0.3	0.4	0.36
Ni	0	0.15	0.06	0	0.15	0.06
Cr	0	0.2	0.03	0	0.16	0.05
Mo	0	0.08	0.02	0	0.08	0.01
V	0	0.01	0.003	0	0.01	0.002
Nb	0	0.005	0.001	0	0.005	0.001
Ti	0.015	0.035	0.022	0	0.014	0.003
Al	0.01	0.035	0.021	0.01	0.03	0.018
B	0.0015	0.0025	0.0018	0	0.0005	0.0001
N	0	0.009	0.0048	0	0.009	0.004
Ca	0	0.01	0.0013	0	0.01	0.0017
Cu	0	0.22	0.14	0	0.25	0.17

In this case B and Ti were the critical elements since they were abundant in the old grade and have stringent restrictions for maximum concentration in the new grade. After casting, two ten-meter-long bars of intermixed steel were downgraded on each line due to the high proportion of B and/or Ti.

Four samples were taken from each downgraded bar of an external line and from each downgraded bar of an internal line. The concentration of each element on these sixteen samples was measured at the centerline, at the surface and at a point placed between them. The resulting concentrations of Ti and B at different points of the bars are plotted on Figure 8. The Figure shows that the differences in the composition of steel across the bar section are not important to determine the intermix region. This validates the assumption of negligible diffusion in the lower part of the line discussed in the previous Section.



(a) B concentration



(b) Ti concentration

Fig. 8--Experimental measurements along the downgraded bars (internal line) for different points of the bar cross section of Example A.

Figure 9 shows (for an external line) the concentration of different chemical elements as function of the length of steel bar cast since the new ladle first opening, at the cut-off point. The continuous lines are the results of the numerical model and the symbols represent experimental measurements. The good agreement observed indicates that the numerical model prescribes correctly the position and length of the intermixed bar.



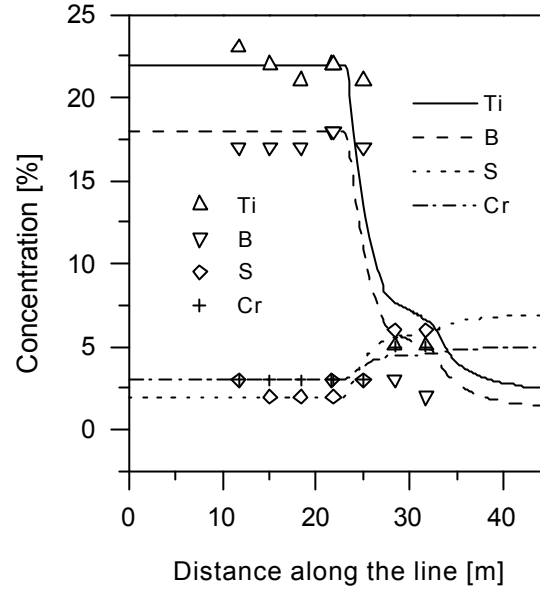


Fig. 9--Numerical results (lines) and plant measurements (symbols) of chemical composition for external line downgraded bars. Four elements were considered: Ti ( $\times 1000$ ), B ( $\times 10000$ ), S ( $\times 1000$ ) and Cr ( $\times 100$ )

#### B. Plant measurements – Example B

The second grade change analysed, is described by Tables IV and V and corresponds to a much longer intermix (six bars were downgraded on each line). Again, four samples were taken from each downgraded bar of an external line and of an internal line. This time, however, only one measurement was performed on each sample. This measurement were taken after forcing the samples, which is the usual procedure carried out in plant to measure steel composition. Thus, the measured concentration is in fact an average of its value across the bar section. In this case Cr and Mo were the more critical elements.

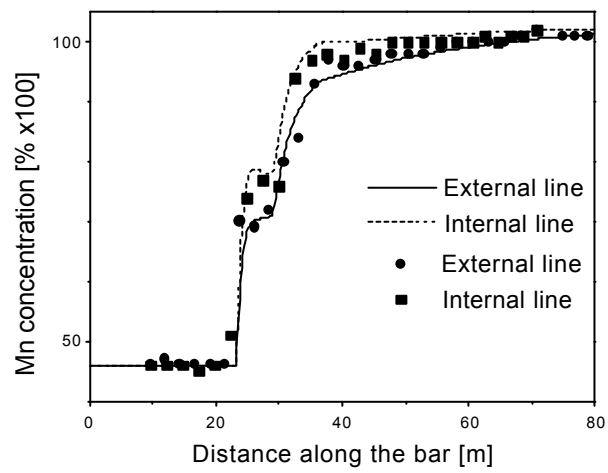
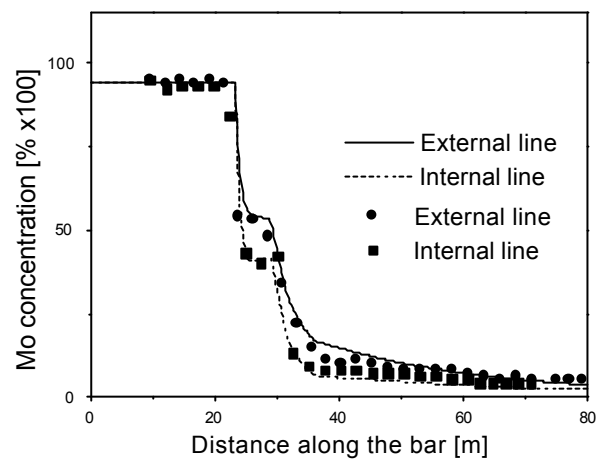
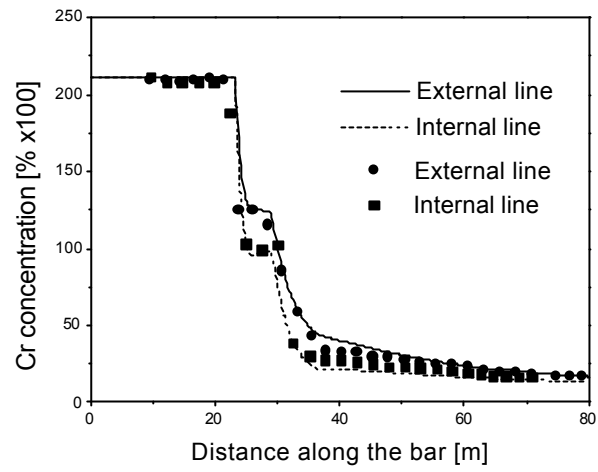
**Table IV. Casting conditions of Example B**

$W_{tundish}$	13.0 tons
$W_{drain}^1$	5.1 tons
$W^1$	7.3 tons
$W_{drain}^2$	5.3 tons
$Q_{steady}$	1.0 ton/min
$Q_{dd}^1$	2.9 ton/min
$Q_{dd}^2$	0.1 ton/min
$Q_{dd}^3$	3.5 ton/min
Bar diameter	0.148 m
Casting speed	2 m/min

Figure 10 shows the numerical results (lines) and the experimental points (symbols) for four different chemical species on the intermixed steel bars. The figure shows that the model is able not only to make a good estimation of the position and length of the intermixed bars, but also to describe accurately the concentration profile along the bars. Even the concentration plateau, due to the ladle closing during the double dilution process, was successfully reproduced.

**Table V. Chemical composition of Example B**

Element	Old Grade		Actual	New Grade		Actual
	Minimun	Maximun		Minimun	Maximun	
C	0.09	0.13	0.12	0.11	0.14	0.13
Mn	0.4	0.5	0.46	1	1.15	1.03
S	0	0.01	0.001	0	0.005	0.005
P	0	0.015	0.01	0	0.02	0.012
Si	0.12	0.23	0.17	0.3	0.4	0.32
Ni	0	0.15	0	0	0.15	0.0
Cr	2.03	2.13	2.11	0	0.16	0.11
Mo	0.92	0.97	0.94	0	0.08	0.01
V	0	0.01	0.005	0	0.01	0.001
Nb	0	0.005	0.004	0	0.005	0.001
Ti	0	0.005	0.002	0	0.005	0.004
Al	0.01	0.035	0.023	0.015	0.04	0.028
B	0	0.0005	0.0001	0	0.0005	0.0001
N	0	0.01	0.0057	0	0.008	0.0048
Ca	0	0.01	0.0024	0	0.01	0.0016
Cu	0	0.15	0.006	0	0.2	0.16



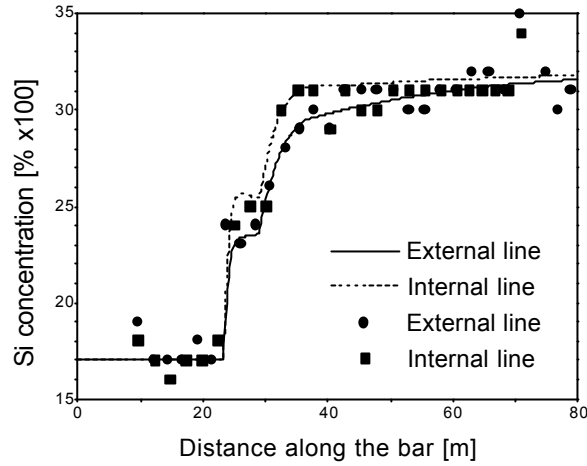


Fig. 10--Numerical results (lines) compared with plant measurements (symbols) for four different chemical elements of Example B.

## VI. TUNDISH FILLING PROCEDURES

To illustrate the advantage of filling the tundish by the double dilution procedure, example B in the previous section is going to be considered again together with a simple dilution procedure example.

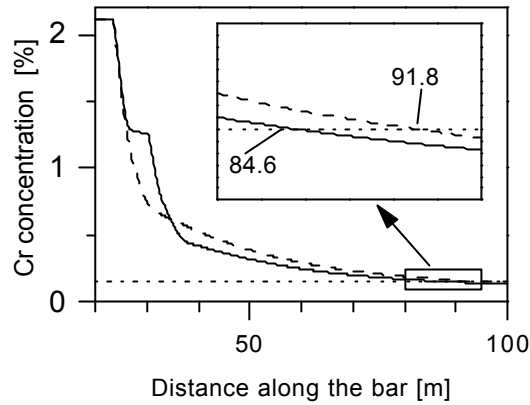
In Section V.B a double dilution procedure was simulated with parameters of Table IV given by real casting conditions. Now, the same grade change (shown in Table V) will be simulated with a simple dilution procedure (Table VI).

**Table VI. Casting conditions of simple dilution**

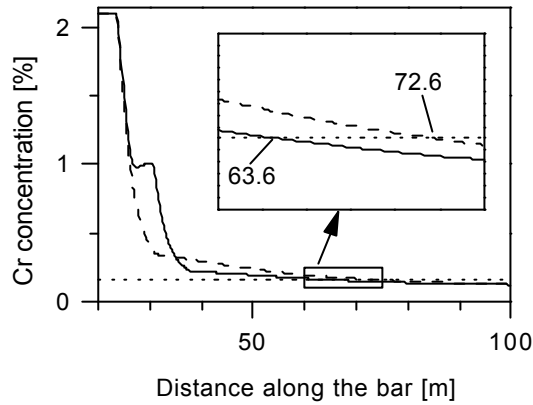
$W_{tundish}$	13.0 tons
$W_{drain}^I$	5.1 tons
$Q_{steady}$	1.0 ton/min
$Q_{sd}$	3.5 ton/min
Bar diameter	0.148 m
Casting speed	2 m/min

Figure 11 shows the concentration of Cr along the bar as calculated by simulating simple dilution and double dilution procedures. The advantage of double dilution procedure becomes evident since its curve reaches the critical concentration before the simple dilution curve does. In this example, 9 m of steel bars are saved on each internal line and 7 m on each external line when a double dilution procedure is

used. A total amount of 4 tons of steel were saved.



(a) corresponds to an external line



(b) corresponds to an internal line

Fig. 11--Concentration of Cr along the bar for the grade transition given by table V. The figure compares results obtained with simple dilution process (dashed line) and double dilution process (full line). The dotted line represents the maximum concentration of Cr allowed in the new grade.

## VII. CONCLUSIONS

The grade transition process at the round billets continuous caster of Siderca was studied and a numerical model was developed. The model provides a fast and accurate estimation of the position and length of the steel bar to be downgraded. The main conclusions of the work are,

1. A methodology to model the mixing in the tundish with several continuous casting lines is presented; in which a defined group of volumes is associated to each line with mixing volumes connecting the different groups to allow recirculation of fluid.
2. The model can simulate different casting conditions including time dependent casting speed and flow rate entering the tundish. In particular, the filling of the tundish in two consecutive steps ("double

dilution” process) was successfully simulated.

3. Double dilution process was found to be more efficient to evacuate the old grade steel remaining in the tundish than the simple dilution process.
4. The short running times and the user friendly interface allows the program to be used practically on line in plant, to indicate where the bars must be cut and to find the optimal sequence of steel grades to be cast.
5. Most of the steel mixing takes place in the tundish. This is probably due to the relatively small volume of liquid steel present on each casting line of the modelled cases, whose diameters are 0.148 or 0.170 m. Besides, diffusion could be neglected in most part of the bar.

### LIST OF SYMBOLS

$C$	Actual concentration of any chemical element
$\tilde{C}$	Actual dimensionless concentration of any chemical element.
$\hat{C}$	Dimensionless concentration in RTD curves.
$C_i^j$	Concentration of any chemical at the exit of volume $V_i^j$ .
$D_{eff}$	Effective diffusivity.
$D$	Molecular diffusivity
$D'$	Turbulent diffusivity
$f_i$	Fraction of the volume $i$
$Q$	Flow rate
$Q_i$	Flow rate between different volumes of the model
$t$	Time
$t_p$	Time delay introduced by plug flow volumes.
$\hat{t}$	Dimensionless time
$V$	Volume, [m <sup>3</sup> ]
$v$	Casting speed
$x_i$	Flow rate fraction
$z$	Distance to the manicus, measured along the bar.
$z_i$	Beginning of the diffusion-convection region.
$z_f$	End of the diffusion-convection region

### Greek Symbols

$\boldsymbol{m}$	Turbulent viscosity
$\boldsymbol{r}$	Steel density
$\boldsymbol{f}$	Bar diameter

### Superscript

$en$	entering the tundish
$ext$	external line
$int$	internal line
$R$	recirculating

### Subscript

$d$	dead
$m$	mixing
$new$	new
$old$	old
$p$	plug

## **ACKNOWLEDGEMENTS**

The authors would like to thank Dr E. Dvorkin for his continuous support in numerical methods.

This research was supported by SIDERCA S.A.I.C., Campana, Argentina.

## **REFERENCES**

1. M.T. Burns, J. Schade, W.A. Brown and K.R. Minor, "Transition model for Armco Steel's Ashland slab caster", *Iron & Steelmaker*, 1992, pp.35-39.
2. X. Huang and B. Thomas, "Modeling of steel grade transition in continuous slab casting processes", *Metallurgical and Materials Transactions B*, 1993, vol. 24, pp. 379-393.
3. X. Huang and B. Thomas, "Intermixing model of continuous casting during a grade transition", *Metallurgical and Materials Transactions B*, 1996, vol. 27, pp. 617-632.

4. H. Chen and R. Pehlke, "Mathematical modeling of tundish operation and flow control to reduce transition slabs", *Metallurgical and Materials Transactions B*, 1996, vol. 27, pp. 745-756.
5. J. Watson, H. Huang and B. Thomas, "Casting dissimilar steel grades", *Steel Technology International*, 1996, pp. 165-170.
6. B.G. Thomas, "Modelling study of intermixing in tundish and strand during a continuous casting grade transition", *Steelmaking Conference Proceedings*, 1996, pp. 519-531.
7. F. Ors, G. Alvarez de Toledo, O. Caballero, E. Lainez and J. Laraudogoitia, "Sequence casting in the production of special steels", *5<sup>th</sup>. European Conference on Continuous Casting*, 1998.
8. F.J. Mannion, A. Vassilicos and J.H. Gallenstein, *75<sup>th</sup> Steelmaking Conference Proceedings*, 1992, vol. 10, pp. 177-186.
9. M.C. Tsai and M.J. Green, *74<sup>th</sup> Steelmaking Conference Proceedings*, 1991, pp. 501-504.
10. A. Diener, E. Görl, W. Pluschkell and K.D. Sardemann, "Mixing phenomena in continuous casting", *Steel Research*, 1990, vol. 61, N° 10, pp. 449-454.
11. D. Martin, M. Ferreyra, J. Madias, A. Campos, G. Walter, E. Rey, E. Guastella and A. Garamendy, "Estudio en modelo de agua del flujo de acero en el repartidor de la máquina 2 de SIDERCA", 1997, IAS Report (in Spanish).
12. M.B. Goldschmit and M.A. Cavaliere, "Modelling of turbulent recirculating flows via an iterative (k-L)-predictor / ( $\epsilon$ )-corrector scheme", *Applied Mechanics Reviews*, 1995, vol. 48, N° 11.
13. M.B. Goldschmit and M.A. Cavaliere, "An iterative (k-L)-predictor / ( $\epsilon$ )-corrector algorithm for solving (k- $\epsilon$ ) turbulent models", *Engineering Computations*, 1997, vol. 14, pp. 441-455.
14. M.B. Goldschmit and R. Javier Príncipe, "Applications of a (k- $\epsilon$ ) model for the analysis of steelmaking processes", *IV World Congress on Computational Mechanics*, Buenos Aires, Argentina, 1998.
15. M.B. Goldschmit, R.J. Príncipe and M. Koslowski, "Numerical modeling of submerged entry nozzle", *3rd. European Conference on Continuous Casting*, Madrid, 1998.
16. M.B. Goldschmit, R.J. Príncipe and M. Koslowski, "Applications of a (k- $\epsilon$ ) model for the analysis of continuous casting processes", *International Journal for Numerical Methods in Engineering*, 1999, vol. 46, pp. 1505-1519.
17. *FANTOM, User manual*, International Center for Numerical Methods in Engineering, (1994).
18. T.J.R. Hughes and A. Brooks, "A theoretical framework for Petrov-Galerkin methods with discontinuous weighting functions: application to the streamline upwind procedure", *Finite Element in Fluids*, 1982, pp. 47-65.
19. A. Brooks and T.J.R. Hughes, "Streamline upwind Petrov-Galerkin formulations for convection dominated flows with particular emphasis on the incompressible Navier-Stokes equations", *Computer Methods in Applied Mechanics and Engineering*, 1982, vol. 32, pp. 199-259.
20. O.C. Zienkiewicz and R.L. Taylor, *The Finite Element Method*. (4<sup>th</sup>. Edition), Mc Graw Hill, London, 1989.
21. *GRADE, User Manual*, Center for Industrial Research, FUDETEC, Argentina.